

Molecular Aggregation Behavior for Binary Monolayer of Fatty Acid ; Effect of Monolayer Structure in a Single Component System

Miyuki Kuramori, Kazuaki Suehiro, and Yushi Oishi

Faculty of Science and Engineering, Saga University, 1 Honjo, Saga 840-8502, Japan
Fax: 81-952-28-8591, e-mail: oishiy@cc.saga-u.ac.jp

The aggregation behavior for mixed monolayer of fatty acids was investigated with respect to the monolayer phase in a single component system on the basis of an atomic force microscopic observation. The surface morphology, the film thickness or the wear property of the monolayers revealed that the (C₁₆/C₂₄) mixed monolayer with the same monolayer phase of L₂ in a single component system and the (C₂₀/C₂₄) mixed monolayer with different phases of LS and CS were in a phase-separated and one phase states, respectively. This result indicates that the aggregation behavior for mixed monolayer of fatty acids is independent of the consistency in monolayer phase in a single component state.

Key words: binary monolayer, fatty acid, monolayer phase, atomic force microscope

1. INTRODUCTION

The increased attention on phase-separated mixed monolayers originates from potential applications as molecular templates for protein crystallization [1] and adsorption [2], patterning layers in molecular photodiode [3] and selective layers in biosensors [4]. These functions depend on the size, distribution and density of phase-separated domains in mixed monolayers. Therefore, a systematic understanding on the phase separation mechanism in a mixed monolayer appears to be an essential step in the design and construction of functionalized structures in a two-dimensional system. The phase separation in a monolayer depends on many factors, for example, difference in cohesive energy between hydrophobic groups, electrostatic repulsion between hydrophilic groups, temperature, surface pressure and so on. Hence, to obtain a general concept of phase separation in a monolayer, it is necessary to investigate a simple experimental system of fatty acid monolayer as a first step.

In this study, the aggregation behavior for binary monolayer of fatty acid with different alkyl chain lengths was investigated on the basis of a microscopic observation with respect to the monolayer phase in a single component system.

2. EXPERIMENTAL

2.1 Monolayer preparation

Palmitic (CH₃(CH₂)₁₄COOH, C₁₆), arachidic (CH₃(CH₂)₁₈COOH, C₂₀) and lignoceric (CH₃(CH₂)₂₂COOH, C₂₄) acids with a purity > 99.99 % were used as monolayer components. Benzene solutions of (C₁₆/C₂₄) and (C₂₀/C₂₄) mixture systems with molar fractions of 100/0, 50/50 0/100 were prepared with a concentration of 8.0 × 10⁻⁴ mol·L⁻¹ except the (C₁₆/C₂₄:100/0) monolayer of 2.0 × 10⁻³ mol·L⁻¹. The sample solution was spread on the water surface at a subphase temperature, T_{sp} of 293 K. After standing for 100 min, the (C₁₆/C₂₄) and (C₂₀/C₂₄)

mixed monolayers were compressed to surface pressures of 7.1 ± 0.5 mNm⁻¹ and 26.5 ± 0.5 mNm⁻¹, respectively, at an area change rate of 8.6 × 10⁻⁵ nm²·molecule⁻¹·s⁻¹ with a microprocessor-controlled film balance system FSD-300 (USI System). The single component monolayers of C₁₆ and C₂₄ at 7.1 mNm⁻¹ were in the same monolayer phase of L₂, whereas those of C₂₀ and C₂₄ at 26.5 mNm⁻¹ were in different phases of LS and CS, respectively [5]. The low-temperature high-pressure phase CS is a two-dimensional crystal of untilted molecules with long-range positional order. This phase corresponds to the historical 'solid film'. The L₂ phase appears at a wide range of temperature and pressures, and the LS phase does at a relatively high temperature and a high pressure. They are hexatic with short-range positional order in which the molecules are tilted toward the nearest neighbor and untilted, respectively. The historical term of the L₂ and LS phases is 'liquid condensed film'.

2.2 Atomic force microscopic observation

Each monolayer was transferred onto a freshly cleaved mica by the horizontal drawing-up method [6] at a transfer rate of 1 mm·min⁻¹. The transfer ratio for each monolayer was unity, indicating that the mica substrate was completely covered by each monolayer. Topographic images of the monolayer surface were obtained with an atomic force microscope (AFM) SPA 300 (Seiko Instruments Industry). The AFM was operated in the constant force mode in air at 293 K, using a 20 μm × 20 μm scan head and a silicon nitride tip on a cantilever with a spring constant of 0.02 N m⁻¹. The applied force during scanning was 6 - 9 nN in an attractive force range. The monolayer thickness was evaluated from the hole depth for an AFM image with a scan area of 1 μm × 1 μm at the minimal force very closely where the probe was pulled off the sample surface, after artificially piercing a hole with an area of 100 nm × 100 nm through the monolayer with the

AFM probe at an applied force of 9 nN in a repulsive force range. The average surface roughness, R_a was designated by the equation

$$R_a = (1/S_0) \int \int |F(x,y) - Z_0| dx dy,$$

where S_0 , Z_0 and $F(x,y)$ are a selected area of $5 \mu\text{m} \times 5 \mu\text{m}$ (in this study), an average surface height in the selected area and a height profile, respectively.

3. RESULTS AND DISCUSSION

3.1 Mixed monolayer with the same monolayer phase of L_2

Figures 1(a) and 1(b) show AFM images of the

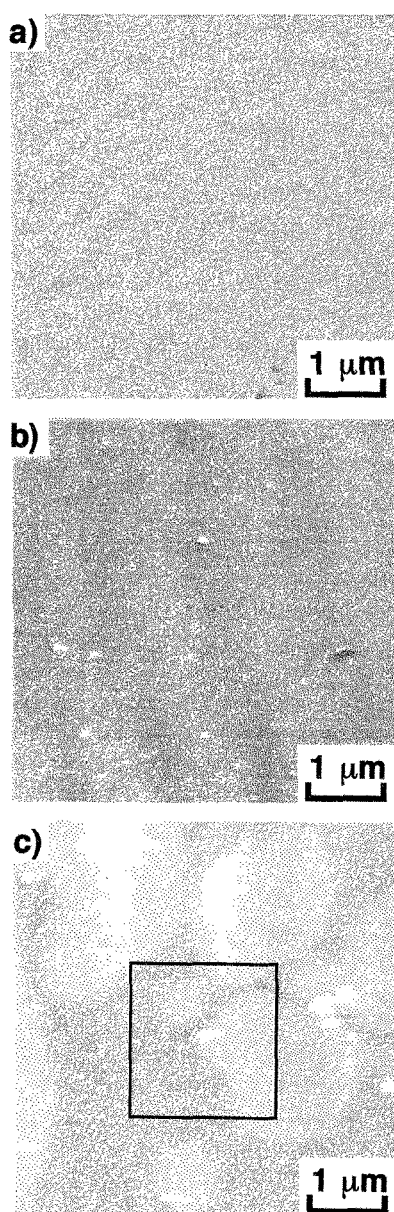


Fig.1 AFM images of the (C_{16}/C_{24}) mixed monolayers with molar fractions of (a)100/0, (b)0/100 and (c)50/50 at surface pressure 7.1 mN m^{-1} on the water surface at T_{sp} of 293K.

palmitic acid (C_{16}/C_{24} :100/0) and the lignoceric acid (C_{16}/C_{24} :0/100) monolayers with a scan area of $5 \mu\text{m} \times 5 \mu\text{m}$, respectively. The surface morphology of the C_{16} and C_{24} monolayers was very smooth with an average surface roughness, R_a of 0.04 - 0.07 nm, excepting holes and aggregates. The film thickness of the C_{16} and C_{24} monolayers were evaluated to be $1.3 \pm 0.2 \text{ nm}$ and $2.5 \pm 0.2 \text{ nm}$, respectively, by piercing a hole through the monolayer. The thickness of the C_{16} and C_{24} monolayers was smaller than the calculated molecular length (1.9 nm and 2.9 nm, distance between carbons of terminal methyl and carboxyl group) of C_{16} and C_{24} of the extended CPK molecular model. It has been reported that the measured thickness of fatty acid monolayers by AFM is often less than the molecular length owing to an AFM probe indentation into a monolayer, depending on the mechanical response of the monolayer [7-12]. The degree of molecular aggregation of the C_{16} monolayer is very low because of the shorter alkyl chain, which causes a deeper indentation of the AFM probe into the monolayer. Hence, the low degree of molecular aggregation for the C_{16} monolayer was probably reflected in the smaller measured value of the film thickness. Another reason for the discrepancy in the monolayer thickness may be sought in the conformation of the alkyl chain. In the case of C_{16} , the weak cohesive force, in other words, the active thermal molecular motion of the C_{16} molecule in the monolayer leads to the introduction of many gauche conformation units into the alkyl chain of the C_{16} molecule. Consequently, the thickness of the C_{16} monolayer truly becomes smaller compared with the calculated molecular length based on the CPK model (all-trans conformation). Figure 1(c) shows AFM image of the (C_{16}/C_{24} :50/50) mixed monolayer with a scan area of $5 \mu\text{m} \times 5 \mu\text{m}$. The observed brighter and darker portions correspond to the higher and lower regions of the monolayer surface, respectively. The surface morphology was heterogeneous in surface height with an average surface roughness, R_a of 0.74 nm, compared with that of the pure C_{16} and C_{24} monolayers. The thickness of the higher domain and

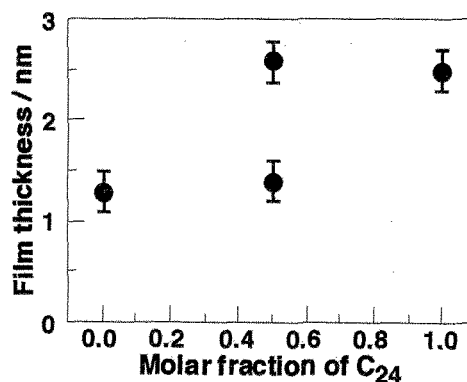


Fig.2 Film thickness of each (C_{16}/C_{24}) mixed monolayer at surface pressure 7.1 mN m^{-1} on the water surface at T_{sp} of 293K.

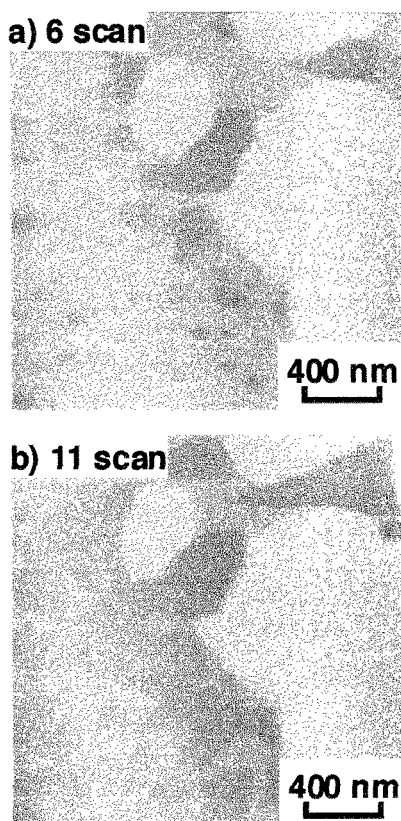


Fig.3 Dependence of the number of scan on surface morphology of (C_{16}/C_{24} :50/50) mixed monolayer.

lower matrix regions agreed with those of the pure C_{24} and C_{16} monolayers, respectively, as shown in Fig.2. And also, the area fraction of the domain and matrix regions agreed with the molar fraction of the spreading solution. These results suggest that the domain and matrix regions are composed of the aggregation regions of C_{24} and C_{16} molecules, respectively. To evaluate the aggregation state of the domains and surrounding matrix, the dependence of the number of scan on monolayer surface was examined. Figures 3(a) and 3(b) show AFM images with a scan area of $2\ \mu\text{m} \times 2\ \mu\text{m}$ after 6 and 11 scans on the marked zone in Fig. 1(c). The area fraction of the darkest portion (the lowest region) corresponding to mica surface increased with the number of scan. Apparently, the repeated scan causes a scratch of molecules in the monolayer, that is, a complete wear. Also, this wear was a selective one of the surrounding matrix region. This suggests that the cohesive force among molecules in the lower regions is weaker than that in the higher regions. Therefore, it is apparent that the (C_{16}/C_{24}) mixed monolayer is in a phase-separated state, and also that the domains and the surrounding matrix are composed of the C_{24} and C_{16} molecules, respectively.

3.2 Mixed monolayer with different monolayer phases of LS and CS

Figures 4(a) and 4(b) show AFM images of the arachidic acid (C_{20}/C_{24} :100/0) and the lignoceric acid

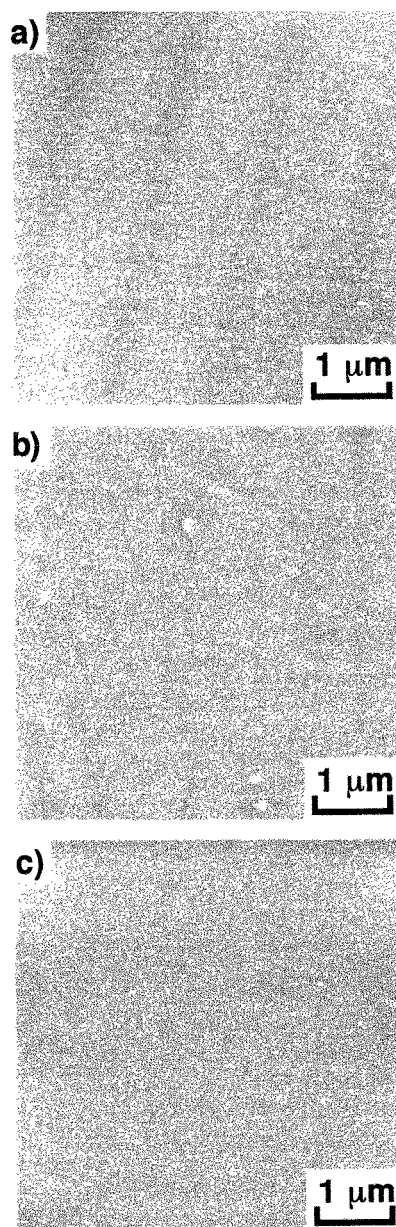


Fig.4 AFM images of the (C_{20}/C_{24}) mixed monolayers with molar fractions of (a)100/0, (b)0/100 and (c)50/50 at surface pressure $26.5\ \text{mN m}^{-1}$ on the water surface at T_{sp} of 293K.

(C_{20}/C_{24} :0/100) monolayers with a scan area of $5\ \mu\text{m} \times 5\ \mu\text{m}$, respectively. The surface morphology of the C_{20} and C_{24} monolayers was very smooth with R_a of 0.13 - 0.14 nm , excepting aggregates of each molecule. The film thickness of the C_{20} and C_{24} monolayers were evaluated to be $2.0 \pm 0.1\ \text{nm}$ and $2.9 \pm 0.1\ \text{nm}$, respectively. The thickness of the C_{20} monolayers was smaller than the calculated molecular length (2.4 nm) of C_{20} of the extended CPK molecular model, although that of the C_{24} monolayer was comparable to the calculated molecular length (2.9 nm) of C_{24} . The smaller thickness of the C_{20} monolayer may result from the probe indentation and/or the conformation of alkyl chain, as discussed

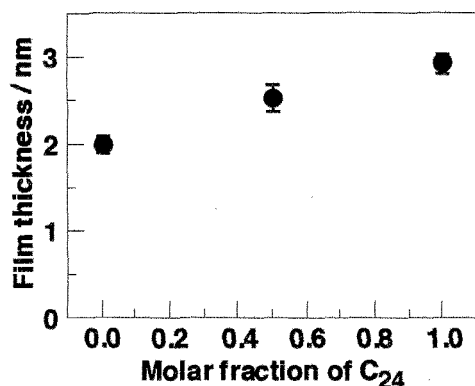


Fig.5 Film thickness of each (C₂₀/C₂₄) mixed monolayer at surface pressure 26.5 mN m⁻¹ on the water surface at T_{sp} of 293K.

for C₁₆ monolayer (Fig.1(a)). Figure 4(c) shows an AFM image of the (C₂₀/C₂₄:50/50) mixed monolayer with a scan area of 5 μm x 5 μm. The surface morphology of the (C₂₀/C₂₄:50/50) mixed monolayer was also very smooth with R_a of 0.20 nm. The film thickness of the (C₂₀/C₂₄:50/50) mixed monolayer was evaluated to be 2.5 ± 0.2 nm. This value was an intermediate one between the film thickness of the C₂₀ and C₂₄ monolayers, as shown in Fig. 5. In the case of a molecular mixing for the (C₂₀/C₂₄) monolayer, the CH₃(CH₂)₃ group corresponding to the difference in molecular lengths of C₂₀ and C₂₄ molecules should stick out and scatter on the monolayer surface. Apparently, the degree of molecular aggregation among the CH₃(CH₂)₃ groups is low, resulting in a large fraction of gauche conformation in the group. This may be reflected in the film thickness of the (C₂₀/C₂₄:50/50) mixed monolayer. The above results exhibit that the (C₂₀/C₂₄) mixed monolayer is in a molecular mixing state.

In principle, like amphiphile mixes like in the monolayer. However, the experimental results in this study is contrary to this principle; the (C₁₆/C₂₄) mixed monolayer with the same monolayer phase in a single component system was in a phase-separated state and also, the (C₂₀/C₂₄) mixed monolayer with different phases was in a molecular mixing one. This discrepancy may result from that the binary system is regardless of the corresponding single component systems owing to a mixing (a complete dispersion of binary components in the spreading solution) before the monolayer formation. The molecular aggregation state of the phase separation for the (C₁₆/C₂₄) mixed monolayer and of the molecular mixing for the (C₂₀/C₂₄) mixed monolayer probably depends on the difference in cohesive energy of alkyl chain in monolayer components [13]. That is, a large difference in the cohesive energy corresponding to eight CH₂ groups (48-60 kJ mol⁻¹) reduces the interaction potential overcoming the entropic contribution, resulting in the phase separation of the (C₁₆/C₂₄) mixed monolayer. On the other hand, a small enthalpic contribution by the difference in

cohesive energy corresponding to four CH₂ groups (24-30 kJ mol⁻¹) causes the molecular mixing of the (C₂₀/C₂₄) mixed monolayer.

4. CONCLUSIONS

The present study suggests that the aggregation behavior of the mixed monolayer is independent of whether the binary components are identical phase or not in a single component state. The mixing behavior depends on the intermolecular interaction, the thermal molecular motion and so on. A further systematic investigation is required to understand the aggregation mechanism in the multicomponent monolayer.

ACKNOWLEDGMENTS

The authors thank Dr. Masao Suzuki (NOF Co.) for providing the samples of palmitic, arachidic and lignoceric acids used in this study. This research was supported in part by a grant from the Ministry of Education, Science and Culture, Japan (Scientific Research (B), Grant No. 09450039).

REFERENCES

- [1] R. H. Newman and P. S. Freemont, *Thin Solid Films*, **284**, 18-23 (1996).
- [2] A. Takahara, K. Kojio, S. Ge, and T. Kajiyama, *J. Vac. Sci. Technol. A*, **14**, 1747-1754 (1996).
- [3] M. Fujihira, M. Sakomura, D. Aoki, and A. Koike, *Thin Solid Films*, **273**, 168-176 (1996).
- [4] B. Fisher, S. P. Heyn, M. Egger, and H. E. Gaub, *Langmuir*, **9**, 136-140 (1993).
- [5] I. R. Peterson, V. Brzezinski, R. M. Kenn and R. Steitz, *Langmuir*, **8**, 2995-3002 (1992).
- [6] Y. Oishi, T. Kuri, Y. Takashima and T. Kajiyama, *Chem. Lett.*, 1445-1446 (1994).
- [7] D. D. Koleske, W. R. Barger, G. U. Lee and R. J. Colton, *Mat. Res. Soc. Symp. Proc.*, **464**, 377-383 (1997).
- [8] A. Schaper, L. Wolthaus, D. Möbius and T. M. Jovin, *Langmuir*, **9**, 2178-2184 (1993).
- [9] L. F. Chi, M. Anders, H. Fuchs, R. R. Johnston, and H. Ringsdorf, *Science*, **259**, 213-216 (1993).
- [10] Y. F. Dufrene, W. R. Barger, J. D. Green and G. U. Lee, *Langmuir*, **13**, 4779-4784 (1997).
- [11] M. Hartig, L. F. Chi, X. D. Liu and H. Fuchs, *Thin Solid Films*, **262**, 327-329 (1998).
- [12] T. Umeda, M. Kuramori, K. Suehiro and Y. Oishi, *Rept. Prog. Polym. Phys. Jpn.*, **42**, 323-326 (1999).
- [13] M. Kuramori, N. Uchida, K. Suehiro and Y. Oishi, *Bull. Chem. Soc. Jpn.*, **73**, 829-835 (2000).